J|A|C|S
ARTICLES
Published on Web 01/13/2007

Residue-Specific $^{13}C'$ CSA Tensor Principal Components for Ubiquitin: Correlation between Tensor Components and Hydrogen Bonding

Robert A. Burton and Nico Tjandra*

Contribution from the Laboratory of Molecular Biophysics, National Heart, Lung, and Blood Institute, National Institutes of Health, 50 South Drive, Bethesda, Maryland 20892

Received September 21, 2006; E-mail: tjandran@nhlbi.nih.gov

Abstract: The residue-specific $^{13}C'$ CSA tensor principal components, σ_{11}, σ_{22}, σ_{33}, and the tensor orientation defined by the rotation angles β and γ have been determined by solution NMR for uniformly labeled ubiquitin partially aligned in four different media. Spurious chemical shift deviations due to solvent effects were corrected with an offset calculated by linear regression of the residual dipolar couplings and chemical shifts at increasing alignment strengths. Analysis of this effect revealed no obvious correlation to solvent exposure. Data obtained in solution from a protein offer a better sampling of $^{13}C'$ CSA for different amino acid types in a complex heterogeneous environment, thereby allowing for the evaluation of structural variables that would be challenging to achieve by other methods. The $^{13}C'$ CSA principal components cluster about the average values previously determined, and experimental correlations observed between σ_{11}, σ_{22} tensorial components and $C'O\cdots H^N$ hydrogen bonding are discussed. The inverse association of σ_{11} and σ_{22} exemplify the calculated and solid-state NMR observed effect on the tensor components by hydrogen bonding. We also show that $^{13}C'$ CSA tensors are sensitive to hydrogen-bond length but not hydrogen-bond angle. This differentiation was previously unavailable. Similarly, hydrogen bonding to the conjugated NH of the same peptide plane has no detectable effect. Importantly, the observed weak correlations signify the presence of confounding influences such as nearest-neighbor effects, side-chain conformation, electrostatics, and other long-range factors to the $^{13}C'$ CSA tensor. These analyses hold future potential for exploration provided that more accurate data from a larger number of proteins and alignments become available.

Introduction

Information regarding chemical shift anisotropy (CSA) is desirable for quantitative determination of dynamics, relaxation interference, and NMR structure elucidation.[1,2] Because of isotropic CSA averaging due to molecular tumbling, solid-state NMR has traditionally been used to investigate the origins of CSA in molecules.[3−11] Additionally, solution NMR values for the ^{15}N and $^{13}C'$ principal components of backbone CSA tensors derived from cross-correlation studies have recently been reported.[12−17] These techniques, while advantageous because the CSA can directly be observed, are only capable of global CSA tensor determination for uniform molecules or under the assumption that all tensors of a similar nucleus are the same. Residue-specific CSA data can be obtained from solution NMR by measuring chemical shift perturbations originating from the anisotropy present under partial alignment in a liquid crystal.[2,18,19] Backbone chemical shifts are subject to influence by a host of physical phenomena such as geometric (torsion angles, side-chain conformation, and hydrogen bonding), solvent (pH and ionic strength), and long-range effects (nearest-neighbor and electrostatics).[1,20−24] These effects must be considered when interpreting the significance of CSA data obtained from solution NMR.

(1) Sitkoff, D.; Case, D. A. *Prog. Nucl. Magn. Reson. Spectrosc.* **1998**, *32*, 165−190.
(2) Burton, R. A.; Tjandra, N. *J. Biomol. NMR* **2006**, *35*, 249−259.
(3) Kiihne, S. R.; Creemers, A. F. L.; Lugtenburg, J.; de Groot, H. J. M. *J. Magn. Reson.* **2005**, *172*, 1−8.
(4) Wei, Y. F.; de Dios, A. C.; McDermott, A. E. *J. Am. Chem. Soc.* **1999**, *121*, 10389−10394.
(5) Wei, Y. F.; Lee, D. K.; Ramamoorthy, A. *J. Am. Chem. Soc.* **2001**, *123*, 6118−6126.
(6) Stueber, D.; Grant, D. M. *J. Am. Chem. Soc.* **2002**, *124*, 10539−10551.
(7) Hartzell, C. J.; Whitfield, M.; Oas, T. G.; Drobny, G. P. *J. Am. Chem. Soc.* **1987**, *109*, 5966−5969.
(8) Sun, H. H.; Sanders, L. K.; Oldfield, E. *J. Am. Chem. Soc.* **2002**, *124*, 5486−5495.
(9) Bower, P. V.; Oyler, N.; Mehta, M. A.; Long, J. R.; Stayton, P. S.; Drobny, G. P. *J. Am. Chem. Soc.* **1999**, *121*, 8373−8375.
(10) Wi, S.; Sun, H. H.; Oldfield, E.; Hong, M. *J. Am. Chem. Soc.* **2005**, *127*, 6451−6458.
(11) Macholl, S.; Borner, F.; Buntkowsky, G. *Z. Phys. Chem. (Munich)* **2003**, *217*, 1473−1505.
(12) Cisnetti, F.; Loth, K.; Pelupessy, P.; Bodenhausen, G. *ChemPhysChem* **2004**, *5*, 807−814.
(13) Loth, K.; Pelupessy, P.; Bodenhausen, G. *J. Am. Chem. Soc.* **2005**, *127*, 6062−6068.
(14) Fushman, D.; Tjandra, N.; Cowburn, D. *J. Am. Chem. Soc.* **1998**, *120*, 10947−10952.
(15) Ying, J. F.; Grishaev, A. E.; Bax, A. *Magn. Reson. Chem.* **2006**, *44*, 302−310.
(16) Hansen, A. L.; Al-Hashimi, H. M. *J. Magn. Reson.* **2006**, *179*, 299−307.
(17) Pang, Y.; Zuiderweg, E. R. P. *J. Am. Chem. Soc.* **2000**, *122*, 4841−4841.
(18) Cornilescu, G.; Bax, A. *J. Am. Chem. Soc.* **2000**, *122*, 10143−10154.
(19) Bax, A. *Protein Sci.* **2003**, *12*, 1−16.
(20) Oldfield, E. *J. Biomol. NMR* **1995**, *5*, 217−225.
(21) Cornilescu, G.; Delaglio, F.; Bax, A. *J. Biomol. NMR* **1999**, *13*, 289−302.
(22) Braun, D.; Wider, G.; Wuthrich, K. *J. Am. Chem. Soc.* **1994**, *116*, 8466−8469.
(23) Le, H. B.; Oldfield, E. *J. Biomol. NMR* **1994**, *4*, 341−348.
(24) Xu, X. P.; Case, D. A. *Biopolymers* **2002**, *65*, 408−423.

Table 1. Experimental and Molecular Alignment Statistics for Ubiquitin under Partial Alignment in Various Liquid Crystal Phases

	bicelles	phage	8% PEG[a]	8% SAG
α (deg)	28.4	144.4	16.4	25.9
β (deg)	32.1	50.3	27.6	36.4
γ (deg)	24.1	48.7	33.1	42.1
Da (Hz)	12.7	9.2	−24.3	−11.1
R	0.61	0.52	0.18	0.60
rmsd D_{NH}[b]	1.1	1.8	3.1	1.3
error $\Delta\delta_N$(meas)	1.4	0.9	1.2	0.9
error $\Delta\delta_C$(meas)	0.3	1.0	1.0	1.2
rmsd $\Delta\delta_N$(meas) − $\Delta\delta_N$(calc)	15.2	12.5	20.5	19.9
rmsd $\Delta\delta_C$(meas) − $\Delta\delta_C$(calc)	9.1	12.1	18.8	14.1

[a] Alignment tensor orientation for 8% PEG was obtained by minimization of the $\Delta\delta_c$ values (see text). [b] All errors and rmsd values are reported in ppb except for D_{NH}, which is reported in Hz.

We report here the residue-specific $^{13}C'$ backbone CSA tensor principal components, σ_{11}, σ_{22}, σ_{33}, as well as the tensor orientation as defined by the rotation angles β and γ. These data were determined using four alignment media—bicelles, Pf1 phage, poly(ethylene glycol) (PEG), and strained polyacrylamide gel (SAG)—and linear regression analysis to correct the experimentally measured shifts for buffer differences between the isotropic and the anisotropic samples. Finally, we investigate and discuss the significance of observed correlations between CSA tensor components and hydrogen bonding.

Results and Discussion

Measurement of D_{NH} and $\Delta\delta_C$. The residual dipolar couplings (D_{NH}) and differences in $^{13}C'$ chemical shift ($\Delta\delta_C$) arising from partial alignment were measured and fit to the high-resolution ubiquitin NMR structure as described previously.[2,18] In each case, the correct molecular alignment for each system was determined by minimization of the difference between measured and calculated D_{NH} values (Table 1). It is not trivial to obtain truly independent alignments with a limited set of media choices.[25,26] Even though the alignments in bicelles and 8% SAG only differ slightly, these data sets can still be used to differentiate among the calculated CSA tensors.

Minimization of the difference between D_{NH}(meas) and D_{NH}(calc) for 8% PEG resulted in a slightly skewed alignment with respect to the $\Delta\delta_C$ values. This error is a result of a comparatively shallow minimum arising from a bias in the 8% PEG D_{NH} population at ∼20 Hz due to a very low rhombicity of 0.18. Minimization of the difference between $\Delta\delta_C$(meas) and $\Delta\delta_C$(calc) produced approximately the same orientation and rhombicity but with a larger magnitude of alignment, −24.3 Hz as compared to −19.4 Hz. To validate this exercise, the same process was applied to the other alignments, and equivalent molecular alignment parameters were achieved whether minimized against D_{NH} or $\Delta\delta_C$ values. Therefore, in the case of 8% PEG, we elected to use the $\Delta\delta_C$ derived molecular alignment parameters.

Correlation between $\Delta\delta_C$(meas) and $\Delta\delta_C$(calc) for ubiquitin aligned with bicelles and phage resulted in rmsd values of 9.1 and 12.1 ppb, respectively (Figure 1). In the cases of alignment with PEG and SAG, initial correlations between measured and calculated $\Delta\delta_C$ values were not acceptable with rmsd values of 37.8 and 37.3 ppb, respectively. Linear regression of D_{NH} values at increasing alignment strengths and extrapolation to zero revealed the theoretical concentration of zero alignment to be 2.1% for PEG and 3.9% for SAG (Figure 2A,B). The observed $\Delta\delta_C$ at these concentrations was then used as the $\Delta\delta_C$ offset at 0% alignment due solely to the variation in buffer conditions between aligned and isotropic samples (Figure 2C,D). Subtraction of these offsets from the observed $\Delta\delta_C$ reduces the rmsd values between measured and calculated $\Delta\delta_C$ to 18.8 and 14.1 ppb for 8% PEG and 8% SAG, respectively (Figure 1).

Plots of the degree of solvent correction for both the $\Delta\delta_C$ and the previously determined $\Delta\delta_N$ onto the structure of ubiquitin are shown in Figure 3. We initially hypothesized that solvent accessibility would be highly correlated to the magnitude of the correction factor. Some regions, such as the N-terminus of the α-helix or the C-terminal β-strand, seem to show some consistency in solvent correction. However, correlation plots reveal no relationship between the magnitude of the required solvent correction and either the alignment medium or the affected nucleus (data not shown). These inconsistencies rule out structural changes as a general influence on the correction factors as one would expect structural effects to lead to similar variations in both ^{15}N and $^{13}C'$ probes. This phenomenon was also observed in our previous attempts to measure CSA in ubiquitin with cetylpyridinium bromide (CPBR)/hexanol. Under partial alignment in CPBR, the D_{NH} rmsd was adequate, 1.1 Hz, yet the $\Delta\delta_N$ rmsd was very high, 95.3 ppb, and the $\Delta\delta_C$ was indeterminable because most of the $^{13}C'$ resonances had disappeared due to line broadening. Therefore, it remains unknown why certain solvent systems affect each nucleus and region to different extents. These observations further confound our current understanding of the CSA and contributing factors.

The resulting corrected $\Delta\delta_C$ values determined as described above are shown in Figure 4. Contrary to the residue-specific $\Delta\delta_N$ data published previously,[2] the $\Delta\delta_C$ values do not show greater uniformity for a given secondary structure segment as dispersion is consistent throughout the length of the protein. This observation suggests that the influence of ϕ and ψ dihedral angles must be smaller on the $^{13}C'$ CSA than on the ^{15}N CSA.

Calculation of Tensor Components. Global average parameters can be evaluated and optimized by numerical minimization of the difference between measured and calculated $\Delta\delta_C$ values while varying the magnitude of the principal components and keeping the orientation fixed. This technique assumes that all nuclei of the same type have the same CSA tensor components and orientation. The average principal component values determined from global Powell minimization and Monte Carlo analysis for σ_{11} (−76.7 ± 0.4 ppm, phage; −62.8 ± 0.3 ppm, PEG; and −79.3 ± 0.2 ppm, SAG), σ_{22} (−8.5 ± 0.2 ppm, phage; −24.9 ± 0.1 ppm, PEG; and −20.3 ± 0.3, SAG), and σ_{33} (85.5 ± 0.1 ppm, phage; 92.8 ± 0.1 ppm, PEG; and 90.2 ± 0.1 ppm SAG) approximate those published previously for bicelles (−74.7 ± 2, −11.8 ± 3, and 86.5 ± 2 ppm for σ_{11}, σ_{22}, and σ_{33}, respectively).[18] It is actually quite surprising given the large difference in buffer conditions and alignment strengths that the values coincide so well.

The principal components of the $^{13}C'$ CSA tensor for each residue can be calculated by minimizing the function $|(\Delta\delta_C\text{(meas)} - \Delta\delta_C\text{(calc)})/\text{error}|$ while varying σ_{11}, σ_{22}, β, and γ as

(25) Ruan, K.; Tolman, J. R. *J. Am. Chem. Soc.* **2005**, *127*, 15032−15033.
(26) Clore, G. M.; Schwieters, C. D. *J. Am. Chem. Soc.* **2004**, *126*, 2923−2938.

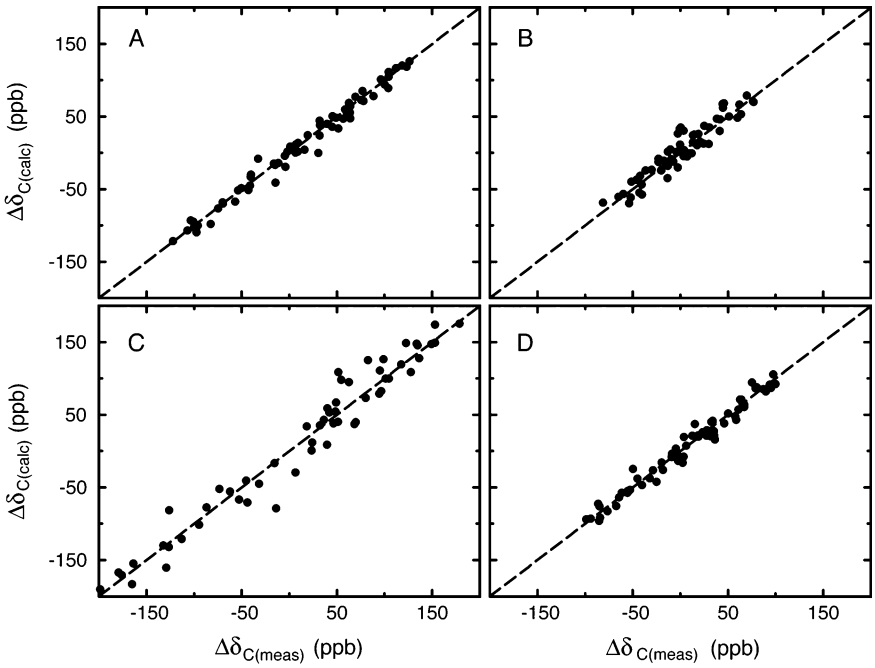

Figure 1. Correlation between $\Delta\delta_C$(meas) and $\Delta\delta_C$(calc) for ubiquitin under partial alignment with bicelles (A), phage (B), 8% PEG (C), and 8% SAG (D) after correction for solvent effect.

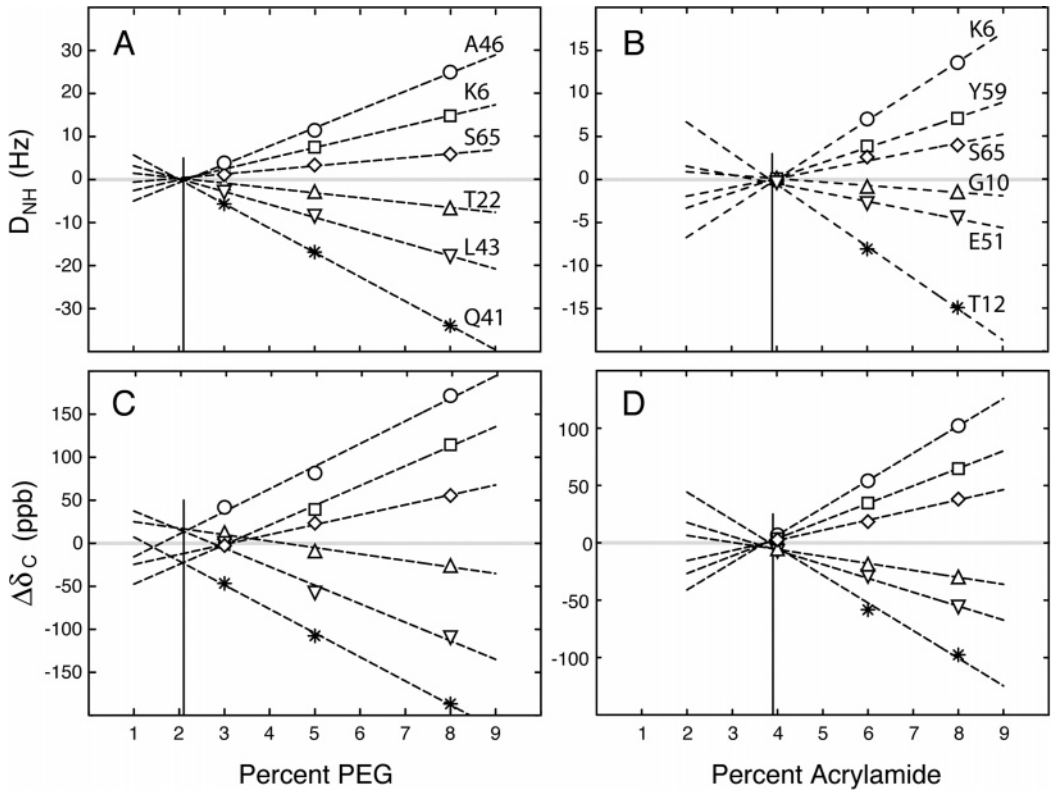

Figure 2. Dependence of D_{NH} (A and B) and $\Delta\delta_C$ (C and D) on percent concentration of PEG and acrylamide. Dashed lines are derived from linear regression and extrapolation of data points for various residues at different alignment strengths. The solid vertical line depicts the theoretical point of zero alignment.

described previously.[2] The σ_{33} component can then be derived based on the traceless relationship with σ_{11} and σ_{22}. The addition of SAG as a fourth alignment system created an extra degree of freedom over that used for the ^{15}N calculations and allowed for the evaluation of the additional rotation angle γ (Figure 5). Previously published data suggest that the size and variation of the Euler angle α is quite small.[7,9,28,29] Therefore, we chose to restrict σ_{22} to the peptide plane.

Despite residue-specific dispersion in the tensor components ($\sigma_{11} = -89.6 \pm 31.3$ ppm, $\sigma_{22} = -6.4 \pm 27.8$ ppm, $\sigma_{33} =$

(27) Koradi, R.; Billeter, M.; Wuthrich, K. *J. Mol. Graph.* **1996**, *14*, 51−55.
(28) Takeda, N.; Kuroki, S.; Kurosu, H.; Ando, I. *Biopolymers* **1999**, *50*, 61−69.

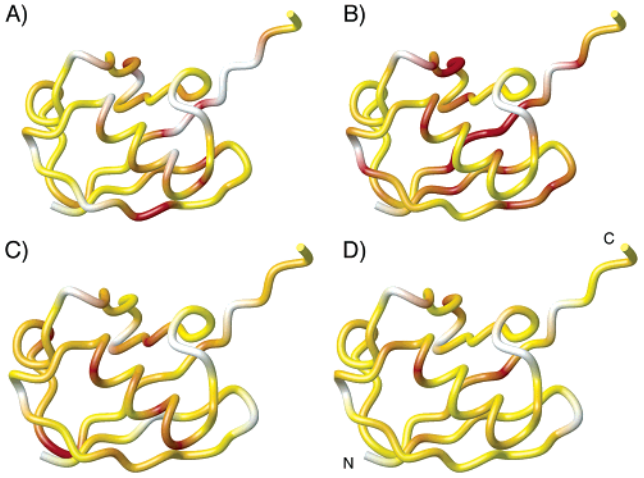

Figure 3. Correction for solvent effect plotted onto the ubiquitin structure for 8% ^{15}N PEG (A) and SAG (B) and 8% ^{13}C′ PEG (C) and SAG (D). The yellow to red color scale indicates increasing magnitude of the required correction. Shifts are defined as follows: yellow = 0−4.9 ppb, orange = 5.0−9.9 ppb, red−orange = 10.0−14.9 ppb, and red >15.0 ppb. No information is available for residues in white, and the N and C termini are labeled in panel D. Figure generated with MOLMOL.[27]

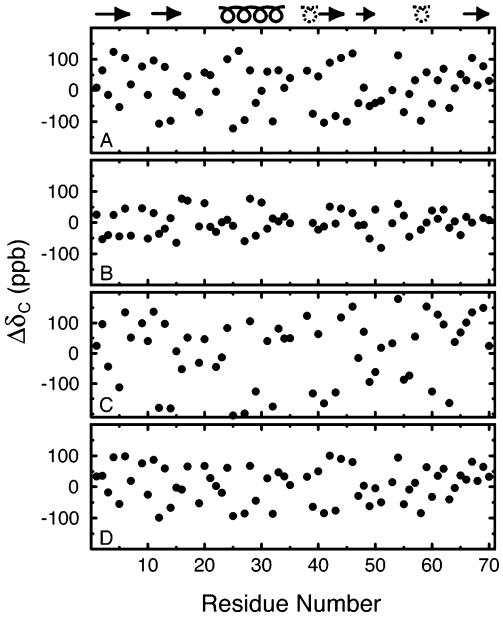

Figure 4. Residue-specific $\Delta\delta_C$(meas) for ubiquitin under partial alignment with bicelles (A), phage (B), 8% PEG (C), and 8% SAG (D). Secondary structure elements are presented above panel A. Arrows indicate β-strands, and coils indicate α-helices. A dotted coil indicates a 3_{10}-helix.

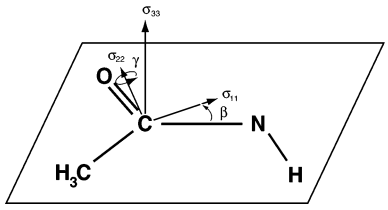

Figure 5. Schematic diagram of the ^{13}C′ CSA tensor principal components, σ_{11}, σ_{22}, σ_{33}, and the tensor orientation angles β and γ.

96.0 ± 37.3 ppm, and β = 33.43 ± 19.1°), most of the components cluster about the averages previously calculated by Cornilescu and Bax,[18] thus confirming the reliability of the experimental data (Figure 6). Also, the newly determined angle γ is generally small (4.0 ± 27.9°), supporting the previous

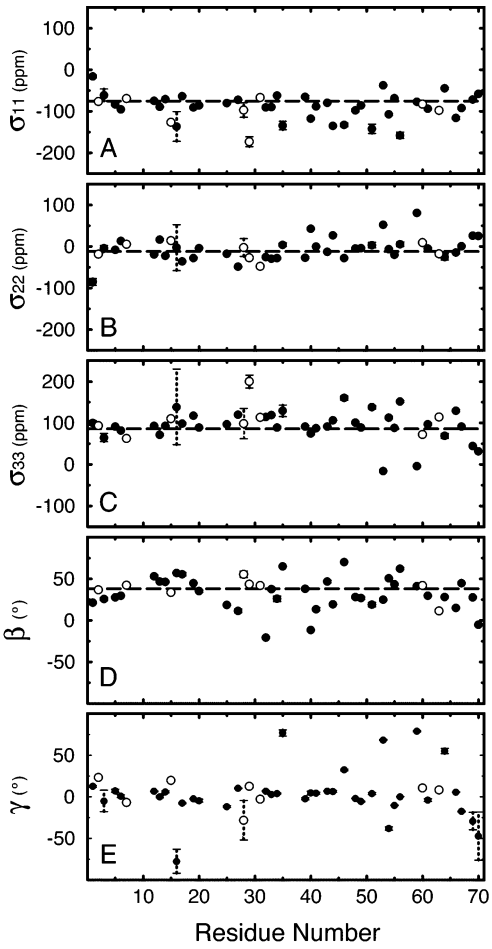

Figure 6. Plots of experimentally determined σ_{11} (A), σ_{22} (B), σ_{33} (C), β (D), and γ (E). Error bars are derived from 40 Monte Carlo simulated data sets, generated by adding Gaussian noise, representative of the error, to the $\Delta\delta_C$(meas). Open circles are data points that yielded a nonzero χ^2 value. Horizontal dashed lines mark the previously determined global averages.

findings from solid-state studies with peptide fragments.[7,29] The dispersion in the tensor components is significant when compared to their average errors (3.84 ppm, 3.95 ppm, 1.11°, and 2.92° for σ_{11}, σ_{22}, β, and γ, respectively). The residue-specific variability indicates that the assumption that all atoms of the same type have the same CSA tensor magnitude and orientation may not be valid for accurate quantitative work.

The difference between the averages calculated by global Powell minimization and those that result from the residue-specific calculation seems to arise from the fact that angles β and γ were fixed to their published values during Powell minimization. The fact that σ_{11} and σ_{22} vary between the two methods but σ_{33} remains fairly constant reveals an inversely dependent relationship between σ_{11} and σ_{22} with respect to β and γ.

Correlations. In much the same manner as before, we attempted to correlate the magnitudes and orientation of the ^{13}C′ CSA tensor principal components with various physical phenomena known to affect CSA, such as secondary structure, ϕ and ψ dihedral angles, *J*-coupling, hydrogen bonding, and primary and secondary chemical shifts of C′, N, and H^N. As with the ^{15}N CSA ubiquitin data,[2] no strong correlations were

(29) Lumsden, M. D.; Wasylishen, R. E.; Eichele, K.; Schindler, M.; Penner, G. H.; Power, W. P.; Curtis, R. D. *J. Am. Chem. Soc.* **1994**, *116*, 1403−1413.

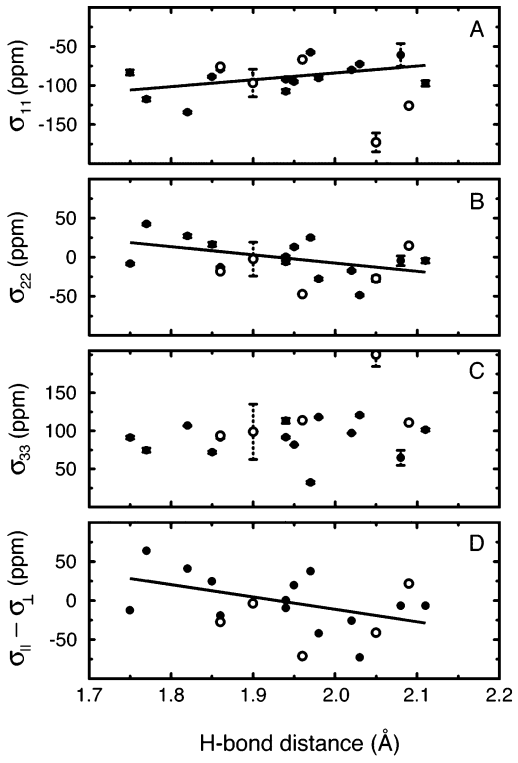

Figure 7. Correlation plots of σ_{11} ($r = 0.5$) (A), σ_{22} ($r = 0.5$) (B), σ_{33} (C), and the parallel−perpendicular components of the $^{13}C'$ CSA tensor ($r = 0.5$) (D) with the C′O···H^N hydrogen-bond length. $\sigma_{||} - \sigma_{\perp}$ was calculated as $(\sigma_{22} - (\sigma_{11} + \sigma_{33})/2)$. Open circles are data points with nonzero χ^2 values and were not included in the regression analysis.

detected between the principle components and any isolated structural factors. As stated previously, strong correlations are not expected due to the quantity and interactive nature of factors that affect CSA. Additionally, because of error in the measurements and the limited sample size, very weak correlations would most likely not be detected. Weak correlations ($r = 0.5$), however, are observed between the $^{13}C'$ σ_{11} and σ_{22} principal components and the C′O···H^N hydrogen-bond length (Figure 7). This analysis only includes residues participating in hydrogen bonds located in secondary structure elements. In this plot, σ_{11} decreases and σ_{22} increases as the hydrogen-bond distance decreases while no change in σ_{33} is observed. The inverse relationship of σ_{11} and σ_{22} and the lack of dependence of σ_{33} leave the isotropic δ_C relatively independent of hydrogen bonding. These data support the previous DFT calculations by Sitkoff and Case on the *N*-methylacetamide dimer that δ_C is unaffected by hydrogen-bond distance but that the quantity ($\sigma_{||} - \sigma_{\perp}$) is.[1] This result would suggest that either σ_{11} or σ_{33} must vary in an opposite sense relative to σ_{22}.

Calculations of the shielding tensors by Kameda et al. support the conclusion that σ_{11} and σ_{22} increase and decrease, respectively, with increasing hydrogen bond length, while σ_{33} remains unaffected.[30] They also showed that δ_C changes with hydrogen-bond length; however, these results may be strongly influenced by backbone conformation as hydrogen-bond lengths are systematically slightly shorter in helices. Wei and co-workers also observed a correlated increase in σ_{22} with decreasing hydrogen-bond length in their solid-state data.[5] In addition, they showed a weaker correlation to the δ_C. Interestingly, somewhat inconsistent with Sitkoff and Case, they did not observe changes in σ_{11} or σ_{33}.

Information regarding the influence of hydrogen-bond angle on the $^{13}C'$ CSA tensor based on ab initio calculations or solid-state studies has not been previously reported. In our studies, neither the $^{13}C'$ CSA tensor magnitude nor the direction was detectably influenced by the hydrogen-bond angle. This observation is a bit surprising considering the strong dependence of the H^N CSA tensor direction with hydrogen-bond angle[31] and is possibly the result of direct participation of the observed ^{1}H nucleus in the hydrogen bond. The much larger, electron-rich character of the oxygen atom may also diffuse the effect of the hydrogen-bond angle on the $^{13}C'$ CSA tensor.

Hydrogen bonding to the $i + 1$ H^N (same peptide plane) also does not visibly affect the tensor components (data not shown). Because of the electronics of the conjugated peptide bond, it is again somewhat surprising that hydrogen bonding at the $i + 1$ H^N does not detectably influence the $^{13}C'$ CSA tensor, especially since the opposite case (influence of C′O···H^N hydrogen bonding on the ^{15}N CSA tensor of the same peptide plane) has been predicted by DFT.[24] These solution data are of additional importance because sample uniformity in previous studies prohibited the differentiation between the influence of hydrogen bonding at the $i/i + 1$ positions.[5,30] In these cases, only the influence of the C′O···H^N on $^{13}C'$ CSA was considered when in fact both C′O···H^N and H^N···O hydrogen bonds were present in the molecules studied. Therefore, the actual source of the influence could not be fully deduced.

Conclusion

The principal components, σ_{11}, σ_{22}, σ_{33}, of the $^{13}C'$ CSA tensor and the tensor orientation via the angles β and γ have been determined for ubiquitin in a residue-specific manner. Averages of the data reported here agree with those determined previously by solid state, cross-correlation, and other partial alignment methods, although the dispersion is quite large. Additionally, the angle γ, heretofore experimentally undetermined for this system, is small, thus confirming previous peptide studies. Together with the previously determined ^{15}N CSA data, these results demonstrate that for quantitative analysis, the assumption that all nuclei of a given type share the same tensor magnitudes and orientation may not be valid.

Correction of inherent $\Delta\delta_C$ and $\Delta\delta_N$ arising from solvent differences between isotropic and anisotropic conditions reveals that the influence of solvent effect on chemical shift is not as straightforward as previously thought. Variations in the magnitude of the required correction are not dependent upon alignment media or the location of observed nuclei. Therefore, the extent of the required correction does not appear to be an obvious result of structural changes or solvent exposure, thus further obfuscating the use of CSA data, determined by measurement of $\Delta\delta$, as an indicator of physical environment at the atomic level.

Weak correlations between the $^{13}C'$ σ_{11}, σ_{22} and the C′O··· H^N hydrogen-bond length were observed, while σ_{33} and δ_C were relatively unaffected. As σ_{22} is parallel to the carbonyl bond, σ_{11} is roughly parallel to the peptide bond, and σ_{33} is normal to

(30) Kameda, T.; Takeda, N.; Kuroki, S.; Kurosu, H.; Ando, S.; Ando, I.; Shoji, A.; Ozaki, T. *J. Mol. Struct.* **1996**, *384*, 17−23.

(31) Sharma, Y.; Kwon, O. Y.; Brooks, B.; Tjandra, N. *J. Am. Chem. Soc.* **2002**, *124*, 327−335.

the peptide plane (Figure 5), one possible explanation for this observation is the change in electronics of the conjugated C′−O and C′−N bonds due to hydrogen bonding. A strong correlation ($r > 0.8$) of these features is not expected due to the multiplicity of factors that influence the magnitude and orientation of the CSA tensor. Other structural influences, such as the ϕ, ψ dihedral angles or hydrogen-bond angle, are most likely weakly correlated in some manner to the ^{13}C′ CSA tensor but are too small or convoluted to be observed in this study.

While much information is theoretically obtainable from detailed experimental analysis of the CSA and the principal components of the CSA tensor, the magnitude and extent of interplay among influencing environmental factors on the CSA remain obscure. We have not considered in our study the influence of primary sequence, side-chain conformations, or long-range effects. Most current CSA data have been deduced based on calculations and solid-state NMR. These techniques have the advantage that the CSA tensor can be directly calculated or observed and evaluated. However, requisite sample simplicity and uniformity limit the extent to which the data are applicable. Solution NMR allows for much more sample complexity, and although effects on the CSA are detected by comparison to δ_{iso}, correlations are still observable. Our results are the first to experimentally differentiate between the interdependence of the ^{13}C′ CSA components with respect to hydrogen-bond length/angle at the $i/i + 1$ position of the carbonyl. Additional efforts are still necessary to deconvolute the impact of these and other factors that affect the CSA principal components. Measurement by solution NMR of the CSA reintroduced by partial alignment is a utile way to approach this problem. Further study on different proteins in additional alignment media will provide the means to evaluate factors other than hydrogen bonding that influence the ^{13}C′ CSA tensor.[35]

Experimental Procedures

NMR Sample Preparation. All samples were prepared with ∼1 mM, purified, uniformly enriched ^{15}N, ^{13}C ubiquitin. Isotropic and anisotropic samples were prepared identically with the exception of the added partial alignment inducing components. Conditions, preparation protocols, and the ^{15}N, ^{13}C, $^{1}H^{N}$ CSA data for the bicelle experiments were published previously.[18] All NMR spectra were recorded at 298 K on a Bruker Avance-800 spectrometer as described previously.[2]

Alignment by phage was achieved in 10 mM KPO_4 pH 6.5, 100 mM NaCl, and 10% D_2O with the addition of ∼15 mg/mL of Pf1 phage (Asla Biotec) as described previously.[2,32] Samples for alignment in 0−8% PEG were prepared in 50 mM NaOAc pH 5.0 and 10% D_2O with the addition of the appropriate amount of $C_{12}E_5$ poly(ethylene glycol) as also described previously.[2,33]

4−10% strained acrylamide gels were prepared by polymerization of the appropriate concentrations of 30% acrylamide/bis-acrylamide, 10% ammonium persulfate, and TEMED (Sigma) in a Teflon casting chamber (New Era Enterprises) with an internal diameter slightly smaller than that of the standard NMR tube.[34,35] After polymerization, the gels were washed in 3 × 2 L of H_2O to remove any non-polymerized materials and then dried at 37 °C overnight. Gels were rehydrated with 50 mM NaOAc pH 5.0 in 10% D_2O and ubiquitin in the Teflon chamber and inserted into NMR sample tubes. The isotropic reference sample was prepared by dissolving 1 mM ubiquitin in 50 mM NaOAc pH 5.0 with 10% D_2O.

Alignment Tensor Calculation. The alignment tensor for ubiquitin in each alignment medium was determined as described previously.[2] For PEG, the target function used in the alignment tensor minimization was $|(\Delta\delta_C(\text{meas}) - \Delta\delta_C(\text{calc}))/\text{error}|$ to overcome the sampling problem introduced by low rhombicity. Powell minimization was used to determine both the global and the residue-specific CSA tensor for ubiquitin. Global CSA tensor determination for each alignment condition was achieved by minimizing the previous function while fixing the β and γ angles to the previously published values of 19 and 11°, respectively, and by assuming that all atoms of a similar type have the same CSA tensor parameters. Residue-specific CSA tensor determination was achieved by altering σ_{11}, σ_{22}, β, and γ for each residue independently to minimize the previous function for all four media simultaneously as discussed previously.[2] To estimate the error, 40 Monte Carlo simulated data sets, generated by adding Gaussian noise, representative of the error, to the $\Delta\delta_C$(meas) were included in each minimization protocol.

Acknowledgment. This work was supported by the Intramural Research Program of the NIH, National Heart, Lung, and Blood Institute.

JA066835C

(32) Hansen, M. R.; Mueller, L.; Pardi, A. *Nat. Struct. Biol.* **1998**, *5*, 1065−1074.
(33) Ruckert, M.; Otting, G. *J. Am. Chem. Soc.* **2000**, *122*, 7793−7797.
(34) Tycko, R.; Blanco, F. J.; Ishii, Y. *J. Am. Chem. Soc.* **2000**, *122*, 9340−9341.
(35) Chou, J. J.; Gaemers, S.; Howder, B.; Louis, J. M.; Bax, A. *J. Biomol. NMR* **2001**, *21*, 377−382.